The Association of Actin and Myosin in the Presence of γ-Amido-ATP Proceeds Mainly via a Complex with Myosin in the Closed Conformation

Werner Jahn*

Abteilung Biophysik, Max-Planck-Institut für Medizinische Forschung, Jahnstrasse 29, D 69120 Heidelberg, Germany

Received February 14, 2007; Revised Manuscript Received May 13, 2007

ABSTRACT: The interaction of γ-amido-ATP (ATPN) and its 2′(3′)-*O*-methylanthraniloyl derivative (mantATPN) with skeletal myosin subfragment 1 (S1) and actomyosin (actoS1) was studied in stopped-flow experiments. Tryptophan fluorescence and fluorescence of the mant label or light scattering were measured simultaneously. Information about the binding of mant nucleotides was obtained from the quenching of tryptophan fluorescence by the mant label. The parameters of various kinetic models were fitted to the experimental traces. The high-fluorescence state of S1 forms with ATPN at a rate of 95 s^{-1} ("open−closed" transition); the transition is only slowly reversible, in contrast to the very fast equilibrium seen with its better known isomer AMPPNP [Urbanke, C., and Wray, J. (2001) *Biochem. J. 358*, 165−173]. The stabilization of the closed state of myosin by ATPN may be due to the formation of a complex with a pentacoordinated amido-γ-phosphate, from which ATPN can dissociate at a rate of 0.005 s^{-1} or be hydrolyzed by cleavage of the $\beta-\gamma$ bond at a rate of 2.5×10^{-4} s^{-1}. A corresponding actoS1−ATPN complex with myosin in the "closed" conformation is the first detectable intermediate in the association of actin and S1−ATPN, giving an experimental access to a state analogous to a key intermediate in the cross-bridge cycle.

The mechanism of muscle contraction involves a cyclic interaction of actin and myosin. Many structural and biochemical details of this cross-bridge cycle have been studied using the soluble myosin subfragment 1, which contains the actin-activated ATPase. The interaction of S1[1] and actoS1 with ATP can be described in a widely accepted kinetic model (Scheme 1; ref *1*).

ATP binds to myosin in a fast reversible step to form a complex which isomerizes almost irreversibly to a state with an increased tryptophan fluorescence (step 2; the degree of fluorescence is indicated by asterisks). Structural studies (*1*) showed this state to be an "open" conformation of the myosin molecule, which is in fast equilibrium (step 3a) with a "closed" conformation with strongly enhanced tryptophan fluorescence (*2*, *3*). The closed conformation represents the enzymatically active configuration (*4*). In the equilibrium 3a the open state is favored, but hydrolysis of ATP (step 3b) is also favorable and the ADP•P_i state is predominantly or exclusively in the closed conformation. Because the equilibrium 3a is very fast, it is not observed as a distinct phase in stopped-flow experiments but affects the magnitude of the observed transient (whose rate corresponds approximately to that of step 3b). The first step in the interaction of ATP with actoS1 is also a fast reversible equilibrium which is followed by an isomerization step (symbolized by a hyphen; step 2′ in Scheme 1b; ref *1*). The dissociation (step 3′) is associated with a change in light scattering and leads to the formation of M*ATP which reacts further according to Scheme 1a. ATP hydrolysis and the transition to the highly fluorescent state occur after dissociation (in solution at high ATP concentration; ref *5*). Most of these kinetic steps have been studied in detail. The state with myosin in the closed conformation, however, is not easily experimentally accessible. Only recently was it recognized that a long-known ATP analogue, γ-amido-ATP (*6*), stabilizes this closed state of myosin. Under steady-state conditions, the enhancement of the fluorescence of S1 with bound ATPN is about 20% higher than the value observed with ATP (*7*). ATPN is the only ATP analogue with a continuous phosphate chain that stabilizes this state. AMPPNP, an isomer of ATPN, is also able to induce an enhanced tryptophan fluorescence of S1, characteristic of the closed conformation. In this case, however, the closed state is present only in a fast equilibrium with the open state, in a ratio of approximately 1:1 (*2*, *3*). Another experimental approach to stabilizing the closed conformation of myosin is provided by the complex with ADP and aluminum fluoride, but this complex forms very slowly and is not well suited to kinetic experiments with myosin. Furthermore, aluminum fluoride interferes with the stability of actin, preventing studies on actomyosin.

In this study, stopped-flow experiments were performed with ATPN and mantATPN with the aim of obtaining more detailed kinetic information. The mant derivative was used, because it was found that binding of mant nucleotides to S1

* To whom correspondence should be addressed. E-mail: Werner.Jahn@mpimf-heidelberg.mpg.de. Phone: (49)-6221-486271. Fax: (49)-6221-486437.

[1] Abbreviations: ATPN, γ-amido-ATP; mant, 2′(3′)-*O*-methylanthraniloyl; AMPPNP, adenosine 5′-(β,γ-imido)triphosphate; S1, myosin subfragment 1; actoS1, S1−actin complex; FRET, fluorescence resonance energy transfer; M, myosin; N, nucleotide; A, actin; P_i/PP_i, inorganic phosphate/pyrophosphate; *m* and m_2, factors determining quench effects at different reaction steps; *n*, number of experiments; SD, standard deviation.

10.1021/bi700318t CCC: $37.00
Published on Web 07/28/2007

Scheme 1

$$\begin{array}{ccccccccc} & & 1 & & 2 & & 3a & & 3b \\ \mathrm{M + ATP} & \leftrightarrow & \mathrm{M{\cdot}ATP} & \leftrightarrow & \mathrm{M^*{\cdot}ATP} & \leftrightarrow & \mathrm{M^{**}{\cdot}ATP} & \leftrightarrow & \mathrm{M^{**}{\cdot}ADP.Pi} \\ & & & & \text{(open)} & & \text{(closed)} & & \text{(closed)} \end{array} \quad (1a)$$

$$\downarrow\uparrow$$

$$\begin{array}{ccccccc} & & 1' & & 2' & & 3' \\ \mathrm{AM + ATP} & \leftrightarrow & \mathrm{AM{\cdot}ATP} & \leftrightarrow & \mathrm{A\text{-}M{\cdot}ATP} & \leftrightarrow & \mathrm{A + M^*ATP} \end{array} \quad (1b)$$

causes quenching of the tryptophan fluorescence, which can be used as an additional signal. Experiments with myosin from *Dictyostelium* showed that this quenching mainly affects tryptophan residues which do not change during the open → closed transition; the fluorescence of the tryptophan(s) signaling this transition is quenched only slightly. Thus, it was possible to get information from the tryptophan fluorescence for both the binding of mant nucleotides and the open → closed transition. The experimental approach was tested by comparing the data obtained from exponential fits to traces of the tryptophan fluorescence with those of the mant fluorescence using the well-studied mant derivatives of ADP and ATP (*8*).

The study revealed the parameters responsible for "stabilizing" the closed conformation of S1 by ATPN and showed that the association of actin with the S1−ATPN complex proceeds mainly via an actomyosin complex in the closed conformation. This complex corresponds to the top of the power stroke, providing an experimental access to this structurally and biochemically still little known state (*4*).

MATERIALS AND METHODS

ATPN was prepared as described (*7*); mantATP, mantdATP, mantADP, and mantATPN were prepared according to ref *9* and purified on a SuperQ (TosoHaas) column using triethylammonium bicarbonate buffer. Nucleotides were analyzed by reversed-phase high-pressure liquid chromatography using a RP18 column with a 10 mM tetrabutylammonium bromide/10 mM phosphate buffer (pH 6.8)−acetonitrile gradient. The identity of the mant nucleotides was confirmed by brief treatment with 1 M NaOH which yielded the starting nucleotides and *N*-methylanthranilic acid. Chymotryptic S1 (from rabbit and chicken skeletal muscle) and actin were prepared by standard methods as described (*7*). The *Dictyostelium* myosin was a construct (GT-M765) having a motor domain identical to that of the wild type. Alkaline phosphatase (calf intestine) was from Roche. Stopped-flow experiments were performed on a Hi-Tech SF-61 DX2 instrument equipped with two photomultipliers and a 75 W Xe/Hg lamp. Intrinsic protein fluorescence and mant fluorescence (via FRET from tryptophan) were excited at 296 nm; 90° light scattering was detected at this wavelength using a band-pass filter (center wavelength 296 nm, 13% transmission; half-width 17 nm; maximum transmission 14.6% at 291 nm). For measurements of tryptophan fluorescence, a band-pass filter (center wavelength 339 nm, 57% transmission; half-width 12 nm; maximum transmission 60.5% at 337 nm) was used. In a few experiments a combination of a WG320 and a UG11 filter (center wavelength of this combination 342 nm, 74% transmission; half-width 34 nm) was used and gave the same results. The tryptophan fluorescence signal in the presence of mant nucleotides was noisy due to the absorption of the exciting light by the mant label, so that up to 25 "shots" were needed at any concentration and the maximal usable nucleotide concentration was about 1.5 mM. Mant fluorescence was detected using a GG455 filter. Curves were fitted to one or two exponential functions using the software provided with the stopped-flow instrument or with the program Origin. For the fitting with differential equations the program Scientist was used, which calculated fits by an iterative procedure using the differential equations appropriate for the model chosen and the squared deviations from the experimental traces as a measure of the goodness of fit. Using Scheme 1c the data from up to ten individual traces could be fitted simultaneously (global fit). In the more complex Scheme 2 (see later), up to seven traces could be fitted simultaneously if steps 1, 2, and 6 were omitted. The differential equations for Scheme 1c were as follows:

$$\mathrm{A + B} \overset{1}{\leftrightarrow} \mathrm{C} \overset{2}{\leftrightarrow} \mathrm{D} \overset{3}{\leftrightarrow} \mathrm{E}$$

$$\mathrm{d}A/\mathrm{d}t = -k_1AB + k_{-1}C$$

$$\mathrm{d}B/\mathrm{d}t = -k_1AB + k_{-1}C$$

$$\mathrm{d}C/\mathrm{d}t = k_1AB - k_{-1}C - k_2C + k_{-2}D$$

$$\mathrm{d}D/\mathrm{d}t = k_2C - k_{-2}D + k_{-3}E - k_3D$$

$$\mathrm{d}E/\mathrm{d}t = k_3D - k_{-3}E$$

$$F = F_0 + \Delta FE/A_0 - (Cm + D + E)\Delta Q/A_0$$

where F = fluorescence, F_0 = fluorescence at time = 0, ΔF = maximal fluorescence enhancement, ΔQ = maximal quench effect, A = [S1], A_0 = [S1] at time = 0, B = [nucleotide], and m = factor by which the tryptophan fluorescence is quenched at step C. In experiments where the nucleotide concentrations used were such that the reaction could be followed to completion, individual curves were standardized so that the final value corresponded to 100% and $\Delta Q = F_0 + \Delta F - 100$. A very slow decrease in the tryptophan fluorescence at the end of the reaction in some experiments (in particular in experiments with mantATP) was neglected. Results were given as the mean, and the SD was given when $n \geq 3$; all experiments were done in buffer M (standard buffer; 100 mM KCl, 5 mM MOPS, 5 mM $MgCl_2$, 0.02% NaN_3, adjusted with Tris to pH 7.0) where not otherwise stated or at low ionic strength (buffer L; 5 mM KCl, 5 mM MOPS, 5 mM $MgCl_2$, 0.02% NaN_3, adjusted with Tris to pH 7.0). Buffer solutions with mantADP were prepared immediately before use to avoid precipitation of the barely soluble Mg^{2+} complex. In experiments with ATPN or mantATPN at concentrations >2 mM the stock solution was complemented immediately before use with equivalent

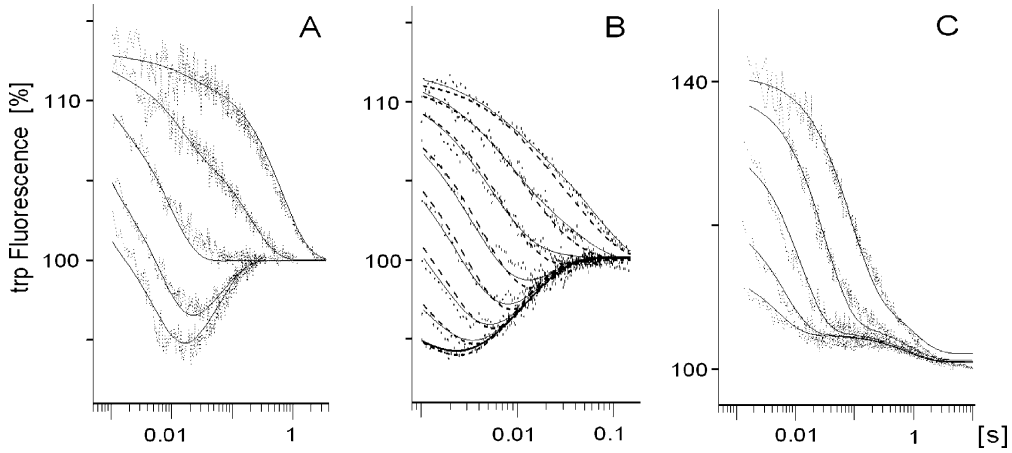

FIGURE 1: Traces of the tryptophan fluorescence (dotted lines) from stopped-flow experiments with S1 and various concentrations (given from top to bottom) of mantATPN (A: 16, 41, 165, 412, 1000 μM), mantATP (B: 4.8, 8.9, 16.5, 33, 60, 113, 227, 467 μM), and mantADP (C: 4.8, 15, 54, 207, 1250 μM); In (A) and (C) only five traces out of ten were shown for clarity. The solid lines represent global fits of the data. In (B) the dashed lines display a global fit with fixed $k_{-2} = 0.001$ s^{-1}.

amounts of Mg^{2+} to compensate for the low affinity of this nucleotide for Mg^{2+} (*7*); traces of ATP or mantATP were removed by treatment with alkaline phosphatase (*7*). Most experiments were performed with rabbit muscle S1A1 or S1A2 at a 1 μM protein concentration (after mixing). Chicken muscle S1 behaved essentially similarly. In actoS1 the ratio of actin:S1 was 1 or 1.5; phalloidin was added routinely at concentrations of 10−50 μM. All concentrations given correspond to the values after mixing. Experiments were done at 20 °C where not otherwise stated.

RESULTS

Amplitudes of Fluorescence Changes Associated with the Interaction of Mant Nucleotides with S1. The interaction of mantATP, mantATPN, or mantADP with S1 led to a quenching of tryptophan fluorescence (Figure 1). High concentrations of mantATP (>30 μM) or mantATPN (>300 μM) induced a fall and a subsequent rise in tryptophan fluorescence (Figure 1A,B), while mantADP induced only a quenching of the fluorescence at all concentrations studied (Figure 1C). The amplitudes of the fluorescence decrease were partially lost because of the dead time of the stopped-flow apparatus. A quantitative comparison of the amplitudes of the tryptophan fluorescence using identical concentrations (5 μM) of the mant nucleotides displayed the highest negative amplitude for mantADP (about 30%; Figure 2, upper part, trace b); the amplitudes of mantATP and mantATPN were about 18% (final value taken as 100%; Figure 2, traces a and c). When the mantATP had been completely hydrolyzed, the same value was reached as was obtained with mantADP. These observations suggest that the change of the tryptophan fluorescence can be viewed as resulting from a quench by about 30% (seen with mantADP alone) and, with mantATP or mantATPN, a fluorescence enhancement of about 15% due to the open → closed transition of S1.

The simultaneously recorded mant fluorescence displayed an increase that was similar in size for all three nucleotides (Figure 2, lower part). There was a very small further increase of the mant fluorescence upon hydrolysis of mantATP (arrow in Figure 2), i.e., during the closed → open transition. When all of the nucleotide had been hydrolyzed, there was a small decrease of the mant fluorescence

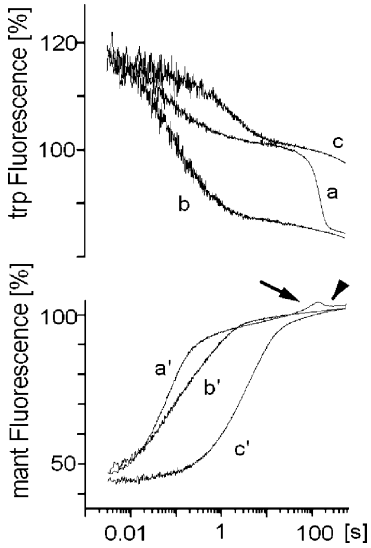

FIGURE 2: Stopped-flow records of the interaction of 5 μM each of mantATP (a, a′), mantADP (b, b′), or mantATPN (c c′) with 1 μM S1. Shown are traces of tryptophan fluorescence (upper part, standardized for a common origin) and of the simultaneously recorded mant fluorescence (lower part, standardized for the end values to correspond to 100%; note the different scale). There is a small increase of the mant fluorescence concomitant to the spontaneous digestion of mantATP (arrow) followed by a decrease of the fluorescence due to the dissociation of mantADP from S1 (arrowhead).

(arrowhead, Figure 2), which can be simply explained by a partial release of mantADP from S1 at this low concentration ($K_D \approx 0.1$ μM; ref *8*).

The displacement of 5 μM mantADP by 80 μM mantATP (Figure 3) showed more clearly the enhancement (about 18%, trace a) of the tryptophan fluorescence during the open → closed transition and the accompanying decrease of the mant fluorescence (trace a′) of about 2%, corresponding to about 6−7% of the total mant fluorescence increase seen on mixing S1 and 85 μM mantATP. In the analogous experiment with equimolar concentrations of mantATPN the increase in the tryptophan fluorescence was slightly larger, and the decrease of the mant fluorescence was slightly smaller (Figure 3, traces b and b′). The drop in mant fluorescence was visible only when a filter with an absorption edge higher than 400 nm was used for the detection of the mant fluorescence signal,

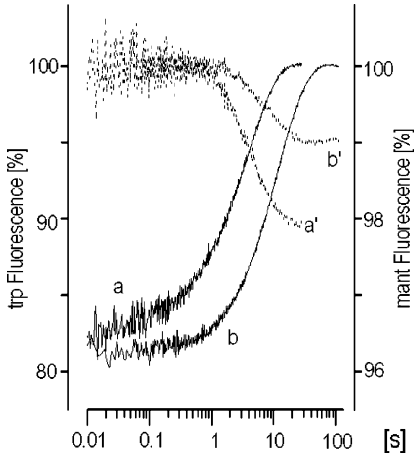

FIGURE 3: Displacement of 4 μM mantADP by 80 μM each of mantATP (a and a′) or mantATPN (b and b′). Shown are traces of mant fluorescence (dotted lines, a′ and b′; starting at 100%) and of tryptophan fluorescence (solid lines, a and b; standardized for the end values to correspond to 100%); note the different scaling.

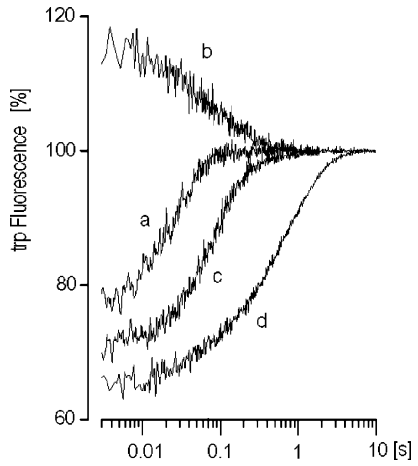

FIGURE 4: Stopped-flow records of the tryptophan fluorescence during interaction of 1 μM *Dictyostelium* mutant protein (GT-M765) with 80 μM mantATP (a), 12 μM mantADP (b), 80 μM ATP (c), or 80 μM mantATP but with previous addition of 4 μM mantADP to the myosin solution (d). Curves were standardized for the end values to correspond to 100%.

since otherwise the effect was hidden by the long-wave edge of the tryptophan fluorescence. This effect was however too small to be used as a signal of the open → closed transition, because it disappeared completely within the global mant fluorescence signal. In contrast to the present observation of a small decrease in the mant fluorescence during the open → closed transition, Woodward et al. (*8*) concluded that the fluorescence increases at this step, perhaps because their comparison of the fluorescence of the mantATP and mantADP states did not consider the slow phase (see below) in the formation of the latter.

In experiments with myosin from *Dictyostelium*, mantATP (concentration range 2−640 μM) led to an enhancement of the tryptophan fluorescence without preceding quenching. The observed fluorescence enhancement was about 15% lower than that seen with ATP (Figure 4, traces a and c), indicating a small quenching of the fluorescence increase associated with the open → closed transition. It is assumed here that the mantADP•P_i and the ADP•P_i states were comparable in occupancy and in the intrinsic intensity of their W501 fluorescence (corresponding to W510 in skeletal myosin), responsible for the fluorescence increase accompanying this transition (*10*). The fluorescence enhancement seen with mantATPN was similar in magnitude to that with mantATP (not shown). In contrast, mantADP induced in *Dictyostelium* myosin a quenching of the tryptophan fluorescence (Figure 4, trace b) which was higher than the difference between the fluorescence enhancements induced by ATP and by mantATP (seen in the displacement experiment in Figure 4, trace d).

These results suggest that the initial quenching of the tryptophan fluorescence on binding of mant nucleotides to skeletal myosin requires the presence of W113 and/or W131, the residues which respond to the binding of ATP or ADP with enhanced fluorescence (*10*) and which are lacking in *Dictyostelium* myosin. In analogy to the observation with *Dictyostelium* myosin, the amplitude of the intrinsic fluorescence enhancement due to the open → closed transition may be influenced only slightly by the quenching effect.

Kinetic Analysis of Stopped-Flow Experiments with Mant Nucleotides. The traces of high concentrations of mantATP and mantATPN could easily be fitted with two exponential functions, yielding a term with a high rate constant and a negative amplitude and a term with a smaller rate constant and a positive amplitude (see above and Figure 1A,B). For the assumed kinetic scheme, the faster rate constant must correspond to binding step(s) while the second represents the open → closed transition. At lower concentrations, the curves rose monotonically but remained biphasic, presumably because the quenched states were reached more slowly and the quench effect overlapped the rise. This case is more fully analyzed below. At low concentrations traces could be fitted to one exponential function. The observed rate constants obtained from the first term reached saturating levels at >1 mM mantATPN, allowing these data to be fitted with a hyperbola, giving $k_2 + k_{-2}$ [Scheme 1a and Scheme 1c (see later)]. The corresponding saturating concentrations of mantATP were reached only at lower temperatures, and the value for 20 °C was extrapolated. For the second term of the exponential function (the tryptophan fluorescence enhancement) saturating levels could be reached with mantATP (giving $k_3 + k_{-3}$, Scheme 1c), but saturation with mantATPN required a concentration so high that measurements were no longer possible.

The tryptophan fluorescence in experiments with mantADP displayed a biphasic quenching effect at all concentrations tested and could be fitted with two exponential functions. The two phases of fluorescence decrease correspond to the two phases of mant fluorescence enhancement reported by Woodward et al. (*8*). These authors observed two phases only up to a concentration of 20 μM mantADP, perhaps because they plotted their results on a linear time scale, where the second exponential fluorescence increase can be overlooked when it is completely separated from the first.

Traces of mant fluorescence (not shown) could be fitted to one exponential function in experiments with mantATP and mantATPN and with two exponentials in experiments with mantADP. The observed rate constants were plotted as a function of concentration, and pseudo-first-order rate constants were calculated for both the tryptophan and the mant fluorescence by linear fits to the initial part of the curves. The results are presented in Table 1 together with

Table 1: Data Obtained by Fitting Exponential Functions to Traces from Stopped-Flow Experiments

$$M + N \xrightarrow{k_1} M^{\dagger}N \xrightarrow{k_2} M^{\dagger\dagger}N \xrightarrow{k_3} M^{**}N^{a}$$

	mantATPN					
	buffer M	buffer L	mantATP	mantdATP	mantADP	ATPN
Trp fluorescence: pseudo-first-order rate constant $\times 10^{-6}$ ($M^{-1}s^{-1}$)	0.8 ± 0.2^{c} ($n = 4$)	2.3 ± 1.3^{c} ($n = 6$)	6.4 ± 1^{b} ($n = 3$)	5.1 ($n = 2$)	2.5 ± 0.2^{b} ($n = 3$)	0.036 ± 0.004^{c} ($n = 4$)
$k_{+3} + k_{-3}$ (s^{-1})	>13	>15	95 ± 10^{c}	>40	1.22 ± 0.05^{c}	98 ± 10^{c}
$k_{+2} + k_{-2}^{c}$ (s^{-1})	400 ± 150	230 ± 50	1200^{d}	~600	215 ± 30	
mant fluorescence: pseudo-first-order rate constant $\times 10^{-6}$ ($M^{-1}s^{-1}$)	0.06 ± 0.02^{b}	0.12 ± 0.03^{b}	2.5 ± 0.2^{b}	2	2.4 ± 0.2^{b}	
$k_{+3} + k_{-3}$ (s^{-1})					1.2 ± 0.1	
k_{diss}^{e} (s^{-1})	0.006	0.006			0.24	0.005

[a] Asterisks and daggers refer to the changes of the tryptophan fluorescence for mantATPN, mantATP, and mantdATP; in experiments with mantADP, step 3 involves a further decrease of tryptophan fluorescence; steps 2 and 3 represent states with enhanced mant fluorescence. [b] Linear fit to initial values. [c] From hyperbola. [d] Extrapolated from experiments at 5, 10, and 15 °C. [e] Displacement rate determined with supramaximal concentrations of ATP.

corresponding data obtained from experiments with mantdATP and ATPN. The values calculated from traces of the mant fluorescence for mantATP, mantdATP, and mantADP are essentially in agreement with published results (*8*). For mantADP, values from measurements of the mant fluorescence were almost the same as those from the tryptophan fluorescence. By contrast, in experiments with mantATP, and even more so with mantATPN, pseudo-first-order rate constants calculated from the two parameters differed greatly. It seems reasonable to assume that in these cases the tryptophan fluorescence was at least partly quenched already at step 1, while the mant fluorescence was not yet influenced at this step.

Global Fitting of Tryptophan Fluorescence Traces. More detailed kinetic information was obtained by global fitting of the tryptophan fluorescence traces using differential equations according to Scheme 1c, which corresponds to Scheme 1a but includes only one step 3:

$$M + N \overset{1}{\leftrightarrow} M^{\dagger}N \overset{2}{\leftrightarrow} M^{\dagger\dagger}N \overset{3}{\leftrightarrow} M^{**}N \qquad (1c)$$

The daggers (†) indicate the decrease (quenching) of the fluorescence. The quenching effect at step 1 was taken into account in the calculations by a factor *m* (see Materials and Methods) which was found to be less than 1 (see below), indicating that a further quenching occurs at step 2, symbolized by two daggers. Constraints for the global fitting were taken from Table 1 as mentioned in the legends of Tables 2 and 3.

Measurements with MantATPN. Results of global fits of experiments under standard conditions and at low ionic strength are shown in Table 2. The corresponding simulated curves of one experiment are displayed in Figure 1A. The SD of the mean values describing the variance between experiments with different S1 preparations was in the range of 10−70% (see Table 2). The mean SD of the data, calculated by the computer program as a measure of the variance within individual experiments, was somewhat smaller. The highest values were found for k_1 (about ±20%) and k_2 (about ±12%). The SD of the other parameters was in the range of 2−6%.

Notable features of the data in Table 2, in comparison with ATP, are the relatively high values for k_{-2} (~70 s^{-1}) and a very low k_{-3}. The latter was identified with the dissociation rate (0.006 s^{-1}) measured by displacement experiments. Since these rate constants are of particular significance, an additional experiment was done to confirm the relationship between these values. In a double mixing stopped-flow experiment, S1 was mixed with mantATPN in a first "shot", followed after an aging time of 0.01−0.03 s by a second mixing with a supramaximal concentration of PP_i (5−10 mM; see ref *7*). The traces obtained (representing the displacement of mantATPN from intermediate states) were compared with simulated curves, using data from Table 2. As shown in Figure 5 the slope of the trace of the tryptophan fluorescence from the double mixing experiment corresponded well to the simulated curve, clearly distinguished from a curve simulated on the basis of a 10 times smaller k_{-2} and a correspondingly 10 times higher k_{-3}. In a control experiment, PP_i displayed no significant influence on the tryptophan fluorescence. The result was confirmed by the simultaneously observed decrease of mant fluorescence and a corresponding simulation on the basis of two global fits of mant fluorescence analogous to Scheme 1c. This simulation was less reliable, because of the fewer data available for mant fluorescence due to the loss of amplitude with increasing concentrations.

Table 2: Rate Constants of the Interaction of MantATPN with S1 Obtained by Global Fitting[a] According to Scheme 1c

	buffer M ($n = 6$)	buffer L ($n = 6$)
$K_1 \times 10^{-3}$ (M^{-1})	1.6 ± 0.4	3.8 ± 1.2
K_2	2.0 ± 0.6	2.3 ± 0.5
$K_3 \times 10^{-3}$	4.7 ± 0.7	4.4 ± 0.4
$k_1 \times 10^{-6}$ ($M^{-1}s^{-1}$)	2.1 ± 0.7	6 ± 4
k_2 (s^{-1})	165 ± 15	136 ± 23
k_3 (s^{-1})	28 ± 5	27 ± 3
ΔF (%)	12 ± 2.5	15 ± 2.5
m	0.9 ± 0.1	0.5 ± 0.1

[a] Constraints used for calculation (lower/upper limit): $k_3 + k_{-3}$ = 15/90 s^{-1}; ΔF = 8/15%. Buffer M: k_1 = 0/5 μM^{-1} s^{-1}; $k_2 + k_{-2}$ = 250/550 s^{-1}. Buffer L: k_1 = 0/10 μM^{-1} s^{-1}; $k_2 + k_{-2}$ = 180/280 s^{-1}.

The reliability of the data obtained from the global fit was confirmed by comparing the association constant calculated from data of Table 2 ($K_{assoc} = K_1K_2K_3 = 1.5 \times 10^7$ M^{-1}) with a value measured by competition experiments with mantATPN and ADP (not shown). A direct titration of S1 with mantATPN could not be performed because of the

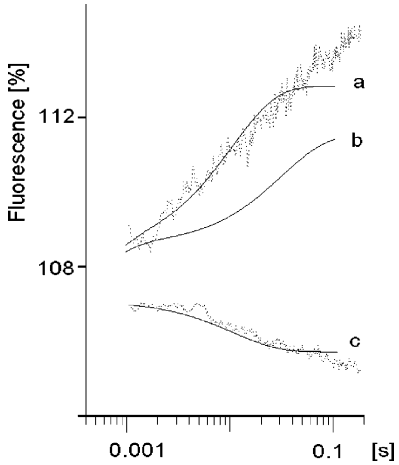

FIGURE 5: Double mixing experiment. In a first step mantATPN (60 μM, final concentration) was mixed with S1. After a reaction time of 0.03 s, PP_i (10 mM) was added in a second step. Shown are experimental traces (dotted lines) of the tryptophan fluorescence (upper curve, a) and of the mant fluorescence (lower curve, c). Superimposed were the simulated traces (solid lines) calculated on the basis of values of Table 2. Line b displays a simulation of the tryptophan fluorescence with a 10 times lower k_{-2} and a 10 times higher k_{-3} to give an impression of the sensitivity of the simulation.

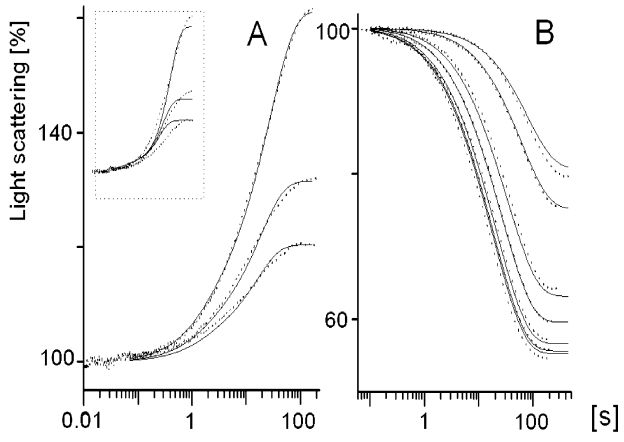

FIGURE 6: Association of actin and S1 (A, dotted lines) and dissociation of actoS1 (B, dotted lines) in dependence of the concentration of mantATPN. (A) 1 μM actin reacted with 2 μM S1 in the presence of 38, 125, or 255 μM ATPN (from top to bottom). The solid lines represent a global fit using individual values for the maximal change of light scattering (ΔS). Insert: global fit using the same ΔS at all concentrations. (B) Dissociation of actoS1 by mantATPN (concentrations from top to bottom: 4.6, 9.2, 45, 91, 250, 500, 760 μM). The solid lines represent global fits calculated according to Scheme 2 without steps 1, 2, and 6.

interference from the enzymatic hydrolysis of mantATPN [$(2-3) \times 10^{-4}$ s^{-1}; this value was found to be the same as estimated with ATPN; ref *7*] with the slow binding rate of mantATPN at low concentrations. It was found that K_{assoc} of mantATPN was 15 times larger than that of ADP. Using a value of $K_{assoc}(ADP) = 10^6$ M^{-1} (*11*) gives $K_{assoc} \approx 1.5 \times 10^7$ M^{-1} for mantATPN, in agreement with the result from the global fit. This association constant may be compared with the corresponding value for ATPN, $K_{assoc} = 0.7 \times 10^7$ M^{-1}, when calculated from K_1k_2 and the displacement rate taken from Table 1. A value of 1.7×10^7 M^{-1} was found in previous experiments under different ionic conditions (*7*). A comparison of the results obtained at standard ionic strength with values observed at low ionic strength (Table 2) revealed a significant difference only in K_1 (and concomitantly in K_{assoc}), which was about twice as high as in standard conditions. This result is in agreement with the expectation that the binding step of mantATPN is essentially dependent on ionic interactions while the isomerization of the protein displays little dependence on ionic strength.

Experiments with MantADP. Fitting of data from mantADP provides a further test of the reliability of the tryptophan fluorescence signal, because only a quench effect was seen, without any interference from the open → closed transition. The M**N state with mantADP in Scheme 1c displays a state of further decreased fluorescence (described in the calculations by a further coefficient m_2 for the amplitude at step 2) and can be symbolized as $M^{†††}N$. One experiment and the fitted curves are shown in Figure 1C. The values obtained from the global fit according to Scheme 1c were ($n = 2$) $K_1 = 1.2 \times 10^4$ M^{-1}, $K_2 = 195$, $K_3 = 4.3$, $k_1 = 25$ M^{-1} s^{-1}, $k_2 = 220$ s^{-1}, $k_3 = 1.03$ s^{-1}; k_{-3} was identified with the displacement rate (0.24 s^{-1}), $m = 0.7$, and $m_2 = 0.89$. The K_{assoc} calculated from these values ($K_{assoc} = K_1K_2K_3 = 10^7$ M^{-1}) was in agreement with published values (*8*) of the dissociation constant (0.1/0.2 μM) calculated from data on the mant fluorescence and from titration experiments. This agreement was not surprising, given that the "conventional" data (Table 1) which were used as constraints were almost identical for mant and for the tryptophan fluorescence. The global fit, however, provided more detailed information. Due to the small value of K_3, there is always a substantial amount of $M^{††}N$ (~13%) in equilibrium with $M^{†††}N$. The fast phase observed on displacement of mantADP by ATP (<10% of the total amplitude) described by Woodward et al. (*8*) may reflect the different displacement rates from the $M^{††}N$ and $M^{†††}N$ states.

Dissociation of ActoS1 by MantATPN or ATPN. The dissociation of actoS1 by mantATPN (Figure 6B) was very slow as was found with ATPN (*7*). The time course of light scattering seen in stopped-flow experiments with ATPN or mantATPN could be satisfactorily fitted only with two exponential functions. Care was taken to avoid interference by traces of ATP in the ATPN stock solution. A kinetic scheme offering a possible description of this situation including the results of association experiments will be given below. In view of the slow dissociation rate, the data from only one shot (which needed up to 10 min) were collected for each nucleotide concentration in the stopped-flow experiments. This was satisfactory for the light scattering traces, which displayed little noise due to the large amplitude. The simultaneously recorded data for tryptophan fluorescence, however, were too noisy to give any reliable information. Qualitatively, tryptophan fluorescence decreased/increased in the experiments with mantATPN/ATPN in parallel to the decrease of light scattering and was not used for calculations. The rate constants of both the fast and the slow component of the double exponential fit of the light scattering traces appeared to saturate at high concentration (>1 mM), giving dissociation rate constants ($k_+ + k_-$) of 0.4 ± 0.1 s^{-1} for the fast component and 0.04 ± 0.01 s^{-1} for the slow component in experiments with mantATPN ($n = 5$). The corresponding values for ATPN were 0.5 ± 0.1 s^{-1} and 0.08 ± 0.02 s^{-1} ($n = 4$). An estimate of the affinity of mantATPN for actoS1 by the method of Siemankowski and White (*12*)

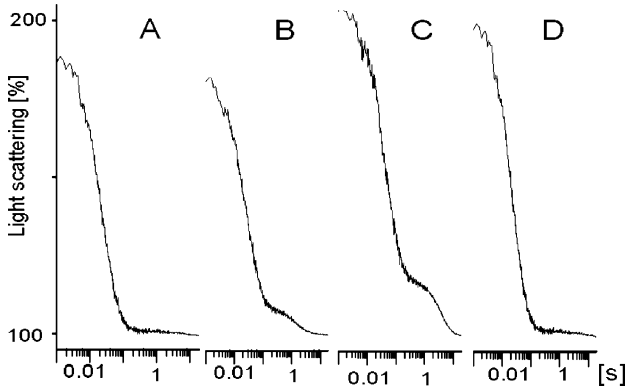

FIGURE 7: Traces of light scattering after mixing of actoS1 (1 μM S1 + 1 μM actin) with 10 μM ATP (A), same experiment 5 min after addition of 1 μM actin to the actoS1 solution (B), after 30 min (C), and same experiment 10 min after further addition of 2 μM S1 to the actoS1 solution (D). These formed a shoulder in the semilogarithmic plot in the presence of excess actin which disappeared after adding an excess of S1.

gave $K_{assoc} = 2.3 \pm 1.3$ mM^{-1} ($n = 6$) under standard conditions and $K_{assoc} = 4$ mM^{-1}($n = 2$) at low ionic strength. These values were within the same range as found for K_1 in Table 2. The corresponding value for ATPN was $K_{assoc} = 0.7$ mM^{-1} in accordance with former measurements (*7*).

Experiments were performed to detect a possible actoS1−mantATPN species with a slow dissociation rate, analogous to the actoS1−mantADP complex that was described by Woodward et al. (*8*) and later reinterpreted as a distinct R-state (*13*). Adding ATP (500 μM) to a mixture of actoS1 and mantATPN (40 μM) revealed a slowly dissociating species (about 13 s^{-1}) seen as a shoulder on the light scattering trace plotted on a logarithmic time scale, without an accompanying change in mant fluorescence. This phenomenon was observed with ATPN also. Surprisingly, the amplitude of this effect increased with the time between the preparation of the actoS1−nucleotide mixture and the start of the experiment (time scale 5−60 min). The shoulder disappeared in the presence of 1 μM S1 in excess over actoS1, which otherwise had little effect on the kinetics of the mantATPN/ATPN−actoS1 interaction. Further investigation revealed this effect to be due to an interaction of actin with actoS1, independent of the presence of nucleotide. Adding actin to actoS1 (prepared as a 1:1 mixture of actin and S1) led to the appearance of a shoulder in the light scattering trace in a time-dependent way during subsequent reaction with ATP. This shoulder disappeared after further addition of S1 (see Figure 7). In the analogous experiments with mantADP, there was a decrease of the mant fluorescence at a rate of 0.4 s^{-1}, observed in parallel to the dissociation. This was interpreted by Woodward et al. as indicating dissociation via a distinct actoS1−mantADP complex, because this fluorescence change was faster than was found by displacement of mantADP from S1 (*8*). The higher displacement rate in those experiments, however, may be due to the competitive interaction of ATP and actin with mantADP•S1 and is not indicative of the dissociation of an actoS1−mantADP species. The simultaneous addition of, e.g., 20 μM actin and 500 μM ATP to mantADP•S1 led to an increase of the displacement rate to about 1 s^{-1} (not shown). On the other hand, the interaction of a very high ATP concentration (5 or 10 mM) with actoS1−mantADP

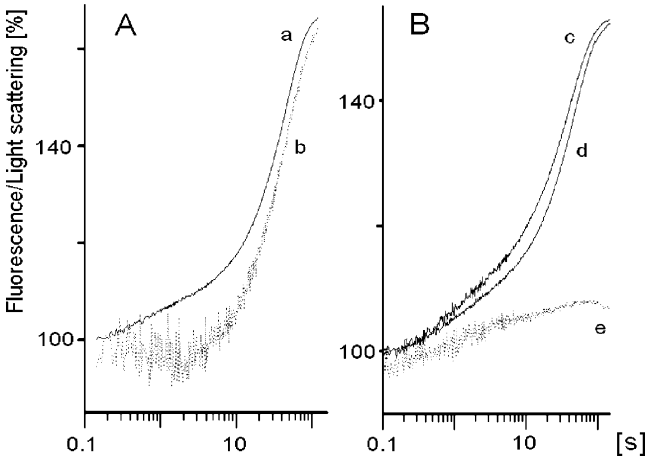

FIGURE 8: Stopped-flow records of the association of actin and S1 in the presence of ATPN (A) or mantATPN (B) at low ionic strength (buffer L). (A) 1 μM actin was mixed with 4 μM S1 and 10 μM ATPN; the upper curve (a) shows light scattering; the trace of the tryptophan fluorescence (lower curve, b) was inverted and the amplitude adjusted to the same level to display the differences more clearly. (B) 1 μM actin was mixed with 10 μM S1 and 39 μM mantATPN; shown are the light scattering (d), the inverted trace of the mant fluorescence (c, amplitude adjusted to the level of the light scattering), and the trace of the tryptophan fluorescence (e, amplitude three times amplified).

led to an increase in the rate of the process underlying the shoulder phenomenon to about 80 s^{-1}, much faster than the rate of the simultaneously recorded displacement of mant-ADP from S1 (about 0.4 s^{-1}, not shown), ruling out any correspondence of the mant signal change with this dissociation step.

Association of Actin with S1−MantATPN or S1−ATPN. The association of actin with S1−ATPN was found to be likewise very slow (*7*). A reevaluation revealed a biphasic process, most clearly seen at low ionic strength (Figure 8). The interaction of S1−ATPN (that is, the S1−nucleotide complex in the closed conformation) with actin led to an increase in light scattering, while tryptophan fluorescence initially remained constant or even rose slightly, followed by a slow further increase of light scattering with concomitant decrease of the tryptophan fluorescence (Figure 8A; the trace of the tryptophan fluorescence was inverted). This shows that S1−ATPN initially binds to actin while still in the closed conformation. In corresponding experiments with mant-ATPN, a biphasic decrease of the mant fluorescence was observed in parallel to the biphasic increase of the light scattering. The trace of the simultaneously recorded tryptophan fluorescence displayed a monotonic fluorescence increase (Figure 8B), which was qualitatively in agreement with the expectation (in analogy to the experiment with ATPN) of an initial decrease of the quenching only due to the decrease of the mant fluorescence, while S1 was still in the closed conformation. The expected higher amplitude of decrease of quenching, concomitant with the second phase of the mant fluorescence decrease, may be partially counteracted by the decrease of the tryptophan fluorescence due to the closed → open transition (seen with ATPN), leading to the monotonic tryptophan fluorescence change.

The described experimental traces were fitted by two exponential functions, and the observed rate constants were plotted. Pseudo-first-order rate constants were calculated by linear fits to initial values (Figure 9). For ATPN the rate

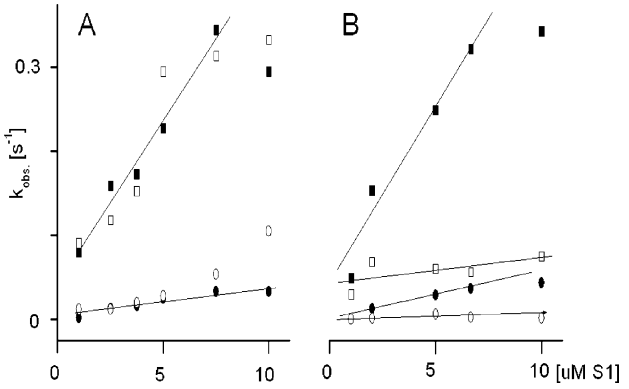

FIGURE 9: Association of 1 μM actin with S1 in the presence of mantATPN (A) or ATPN (B). Experimental traces were fitted by two exponential functions, and the observed rate constants were plotted in dependence of concentration of S1 (high rate constants, rectangles; low rate constants, circles). (A) Observed rate constants of light scattering (filled symbols) and of mant fluorescence (empty symbols); the pseudo-first-order rate constants obtained from linear fits to initial values (straight lines) were the same for both parameters (3.9×10^4 and 0.5×10^4 M^{-1} s^{-1}). (B) Observed rate constants of light scattering (filled symbols) and of tryptophan fluorescence (empty symbols); the pseudo-first-order rate constant from the linear fit of the fast rate constants of the light scattering was almost the same as found for mantATPN (4.4×10^4 M^{-1} s^{-1}), while the corresponding rate constant from traces of tryptophan fluorescence (0.3×10^4 M^{-1} s^{-1}) was within the range of the value obtained from the lower rate constants of the light scattering (0.6×10^4 M^{-1} s^{-1}). The value from the lower rate constants of the tryptophan fluorescence was 0.6×10^3 M^{-1} s^{-1}.

Scheme 2

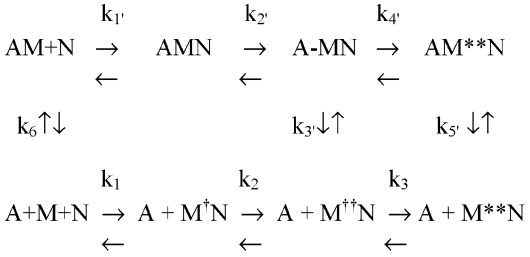

constants measured on the basis of light scattering were clearly different from values obtained on the basis of tryptophan fluorescence (Figure 9B), while the rate constants calculated from values of light scattering or mant fluorescence were almost the same in experiments with mantATPN (see legend to Figure 9A).

These experiments (Figure 8) show that the AM**ATPN complex is the first detectable step in the association of actin and M**ATPN and therefore a step in the dissociation as well (for thermodynamic reasons). Thus, Scheme 1b is not sufficient to describe the association and dissociation of actomyosin by ATPN and must be supplemented with additional steps. This is done in Scheme 2, which extends Scheme 1b to include step 4′ and combines it with Scheme 1c. This scheme contains the minimum of steps necessary to describe the present data. Possible collision complexes were omitted. Since steps 1 and 1′ both represent fast equilibria, any interaction between AMN and A + M†N would be of little kinetic relevance and was neglected. Anyway, since $K_1 \approx K'_1$ the corresponding equilibrium constant would be of the same magnitude as K_6, and this simplification would be of little influence.

Global Fitting of Light Scattering Traces. Scheme 2 (without steps 1, 2, and 6) was used as the basis for global fits of the traces of light scattering of actoS1 dissociation by ATPN/mantATPN and for the association of actin and S1 with ATPN or mantATPN bound. Values for steps 3 and 1′ ($\approx$1) were taken from Table 2. The latter was an approximation, since the equality of $K_{1'}$ and K_1 does not imply identical rate constants. There were not enough constraints available to completely define the cyclic reaction scheme. In view of the impossibility of obtaining definite values solely on the basis of the data presented, most of the values shown in Table 3 are given as ranges. From the association experiments, the reaction appeared to proceed mainly via steps 5′ and 4′, rather than via steps 3 and 3′, justifying the use of the rate constants found for the dissociation ($k_+ + k_-$; see above) as starting values for $k_{4'} + k_{-4'}$ and $k_{5'} + k_{-5'}$ in the calculation. The results obtained in this way with mantATPN are shown in Table 3. A check on the reliability of these values could be obtained from a calculation of K_6 according to the complete Scheme 2, using the data of mantATPN from Tables 2 and 3. From detailed balance, $K_6 = K_2/K_{2'}K_{3'}$ (since $K_1 \approx K_{1'}$), which gives $K_6 \approx 3 \times 10^8$ M^{-1} as a rough estimate. This value is higher by a factor of 30 than is expected at this ionic strength (*14*). Nevertheless, this result seems not to be completely unreasonable in view of the very indirect method of estimation and the mean variation of the data. The fit of experimental traces is compatible with a wide range of values for individual rate constants. The equilibrium constants, however, are much less influenced by the variation of these values. A change of $k_{5'}$, for example, from 0.4 to 5.5 s^{-1} causes a change of $K_{3'}$ from 1.3×10^{-3} to 1.8×10^{-3} μM^{-1}. The values from experiments with unlabeled ATPN and actoS1 were similar in magnitude to those found with mantATPN (see Table 3).

The rate constants obtained from global fit of the dissociation experiments should describe the association as well. The traces from association experiments in the presence of mantATPN were fitted using $K_{1'}$ and $K_{2'}$ from dissociation experiments as fixed values. The calculated values of the other rate constants were not in complete agreement with the results of the dissociation experiments (Table 3). Global fits with various starting values gave an approximate upper limit of about 1 s^{-1} for $k_{5'}$, while fits to the dissociation experiments were compatible also with higher values for this rate constant (not shown).

Several experiments were done to elucidate possible reasons for the discrepancies between the data found for the association and the dissociation. Since reaction rates of dissociation were in the range of the spontaneous dissociation rate of actoS1 (0.2 s^{-1}; ref *15*), the light scattering signal, which is sensitive to the shape of the proteins, may be influenced by a redistribution of S1 on the actin filament during the dissociation or association. Information on the magnitude of this effect was obtained by mixing 1 μM actoS1 with 5 μM actin. This led to a decrease of the light scattering of about 5% (Figure 10) at a rate similar to that found for the displacement of pyrene-labeled actin from actoS1 with actin (see ref *15*). This rate could be measured only approximately because the decrease of light scattering was immediately followed by a strong increase apparently due to aggregation phenomena (*16*). This result is, in principle,

Table 3: Results from Global Fit of Stopped-Flow Experiments of Dissociation of ActoS1 and Association of Actin and S1 in the Presence of MantATPN or ATPN According to Scheme 2 but Omitting Steps 1, 2, and 6

	mantATPN		ATPN	
	dissociation[a] ($n = 4$)	association[b] ($n = 2$)	dissociation[b,c] ($n = 2$)	association[b] ($n = 2$)
$K_{1'}$ (μM^{-1})	$\{1.6 \times 10^{-3}\}$ ($\approx K_1$)	$\{1.6 \times 10^{-3}\}$	$\{0.7 \times 10^{-3}\}$	$\{\sim\}$
$K_{2'}$	5.5 ± 1.5	$\{\sim\}$	6/1	16/3
$K_{3'} \times 10^3$ (μM)	1.3 ± 0.4	1.7/0.7	1/0.4	0.8/0.3
$K_{4'}$	0.05 ± 0.04	0.3/0.2	4/0.4	1.5/0.1
$K_{5'}$ (μM)	175 ± 150	32/8	50/6	30/8
$k_{2'}$ (s^{-1})	39 ± 12	$\{\sim\}$	200/2	16/1
$k_{3'}$ (s^{-1})	0.16 ± 0.06	0.008/0.005	8/0.3	0.5/0.05
$k_{4'}$ (s^{-1})	0.002 ± 0.001	0.05/0.02	0.5/0.02	0.06/0.01
$k_{5'}$ (s^{-1})	0.38 ± 0.01	0.9/0.3	5/0.4	0.5/0.2

[a] K_1, k_3, and k_{-3} were taken from Table 2. [b] The pairs of numbers represent high and low values obtained from several calculations per experiment with various starting values; calculations were in compliance with detailed balancing, but of course not all combinations of values shown fulfill this requirement. [c] $K_{1'}$ was estimated according to ref *12*; k_3 and k_{-3} were taken from Table 1 ($k_3 \approx k_3 + k_{-3}$; $k_{-3} = k_{diss}$); values fixed during calculation are shown in braces ({ }); $\sim$ values were taken from dissociation experiments; the global fit of dissociation experiments was on the basis of seven individual traces each time; the calculations of association experiments were on the basis of four to six traces.

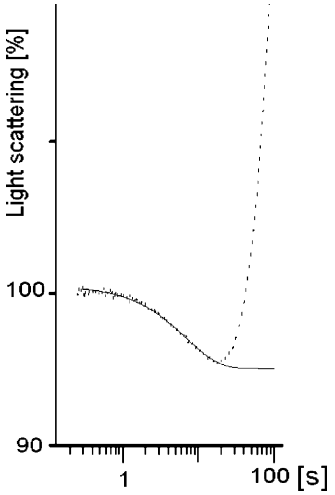

FIGURE 10: Record of the light scattering after mixing 1 μM actoS1 with 5 μM actin in a stopped-flow experiment (dotted line). The solid line is an exponential fit to the initial part of the trace; observed rate constant, 0.2 s^{-1}.

in agreement with the finding of Blanchoin et al. (*17*) in that the light scattering by F-actin saturated with S1 is more intense than for the same concentration of actoS1 in the presence of excess actin. Given this result, a true linear relation between dissociation or association and light scattering is not to be expected, in particular at low reaction rates and with low amplitudes. A further indication of a nonlinear relation between light scattering and the degree of association was observed by global fitting of traces of association experiments at constant protein concentration but in dependence on nucleotide concentration. In these calculations the value of the maximal increase of the light scattering (ΔS) should be the same for all nucleotide concentrations. However, calculations could be done properly only with individual values for this parameter for each nucleotide concentration (see Figure 6A).

Experiments with MantATP and MantdATP. The investigation of the tryptophan fluorescence in experiments with mantATP was of particular interest for methodological reasons. Global fits were calculated according to Scheme 1c using values for $k_2 + k_{-2}$ and $k_3 + k_{-3}$ from Table 1 as constraints. This calculation led to $K_1 = (8 \pm 0.6) \times 10^3$ M^{-1} and $k_1 = (1.7 \pm 0.7) \times 10^7$ M^{-1} s^{-1} ($n = 4$). The calculated value of K_2, however, was unacceptably low ($\approx$20; $k_2 \approx 1200$ s^{-1}) given that this step is almost irreversible. Fitting with k_{-2} fixed at a low value (0.001 s^{-1}), to examine the effect of this parameter on the calculated curve, led to a moderate increase (about 70%) in the mean error, measured as the sum of squared deviations. The corresponding curves were still within the noise of the experimental traces (see Figure 1B). These experiments reveal a limitation on the use of the data from the quenching of tryptophan fluorescence. If the relation of the rate constants is such that major changes have only a subtle effect on the shape of the fluorescence traces, it may be impossible to get reliable results.

Due to the acyl migration on vicinal diols, mantATP is an equilibrium mixture of the 2′-isomer (35%) and the 3′-isomer (65%; ref *18*). If these isomers display very different quenching efficiencies, small kinetic differences could induce a complexity in the experimental traces which may be responsible for problems in critical situations, e.g., the calculation of k_{-2}. Experiments with analogues of the 3′-isomer, mantdATP and mantdADP, showed that the quenching effect of mantdADP was almost equal to that for mantADP. The quenching effect on binding of mantdATP, however, was larger than with mantATP; correspondingly, the difference between the quenching effect of mantdADP and the quenching effect of mantdATP, i.e., the fluorescence enhancement (ΔF) associated with the open $\rightarrow$ closed transition, was about half of that seen with mantADP/mantATP. Global fitting of mantdATP traces led to values similar to those obtained with mantATP, except for k_2 and k_3 ($K_1 \approx 10^4$ M^{-1}, $k_1 \approx 2.4 \times 10^7$ s^{-1} M^{-1}, $K_2 \approx 30$, $k_2 \approx 610$ s^{-1}, $k_3 \approx 40$ s^{-1}; $n = 2$).

The global fit of simulated traces corresponding to the interaction of S1 with a mixture of 65% mantdATP ($\Delta F =$ 6%) and of 35% of a species with a $k_2 = 2400$ s^{-1} and $\Delta F = 12\%$ but otherwise unchanged parameters revealed standard deviations of the calculated rate constants k_1, k_2, and k_3 of 1−2%, clearly smaller than those observed with experimental traces. On the basis of this result, the inhomogeneity of the mant nucleotide(s) in respect to the position of the mant label appears to have little effect on the variance of the data.

In dissociation experiments with actoS1 and mantATP, the pseudo-first-order rate constants obtained from the plot of the observed rate constants of tryptophan fluorescence were almost the same ($6.9 \pm 2 \times 10^6$ M^{-1} s^{-1}; $n = 5$) as in

experiments with S1 alone (see Table 1). This indicates that the quenching of the tryptophan fluorescence occurs in the same way in actoS1 as in S1. The saturating level for $k'_2 + k'_{-2}$ (Scheme 1b) was beyond the limit of measurement, while the saturating value of the dissociation rate measured by light scattering ($k_{3'} + k_{-3'}$) was of the same magnitude (390 ± 40 s^{-1}; $n = 5$) as a published value (388 s^{-1}; ref *8*). The value of $k_3 + k_{-3}$ did not differ significantly (84 ± 4 s^{-1}; $n = 5$) from that with S1.

DISCUSSION

A substantial result of the present study is the observation of a relatively slow transition from the open to the closed myosin S1 state and a very slow rate of the backward reaction (k_{-3}; Scheme 1c). In experiments with mantATPN, k_{-3} was identified with the displacement rate. This identification seems reasonable also for the unlabeled ATPN, because the experimental results for the labeled and the unlabeled nucleotide were similar, as were results for mantATP and mantADP (*8*). A slow transition between M*N (M††N) and M**N states is unexpected, because it is known from temperature and pressure jump experiments that this transition is very fast (rate constants within the range of 800−2000 s^{-1}), when N is ATP, AMPPNP, or the ADP−beryllium fluoride complex (*2*, *3*). There appears to be a fundamental difference between these states and the M**ATPN state. This is surprising, because ATPN differs structurally from ATP less than does its chemical isomer AMPPNP, which displays a slightly changed geometry of the phosphate chain in comparison with ATP due to the bridging NH group between the β- and γ-phosphates. Steric factors seem unlikely as a reason for the slow transition. The rate of the open → closed transition found with ATPN is close to the rate of the transition of the M*ATP state to the M**ADP.P$_i$ state, suggesting that the M**ATPN state may be analogous to the M**ADP•P$_i$ state. For the latter state, a pentacovalent γP$_i$ with an unbroken $\beta-\gamma$ bond has been discussed (*1*), and the chemical properties of ATPN may allow it to form an analogous pentacoordinated state. The large difference in the behavior of ATPN and ATP would then be caused by the different stabilities of the M**ATPN and M**ADP•P$_i$ states. The transition from the M**ADP•P$_i$ state to the M*ATP state (via M**ATP) is relatively fast ($k_{-3} = 10$ s^{-1}). In contrast, ATPN appears to be more strongly bound in the pentacoordinated state and can be released from this state at a rate of 5×10^{-3} s^{-1}. It is not clear whether the primary transition product is another "M**ATPN" state in the closed conformation (just without the pentacoordination at the γP) analogous to the M**ATP state or whether there is a transition directly to the M*ATPN state. In the former case, the expected fast equilibrium M*ATPN ↔ "M**ATPN" would have to be far to the left, because of the large amplitude of the fluorescence enhancement seen in the stopped-flow experiments and because no transient is seen in T-jump experiments (*7*). If, as hypothesized here, the M**ATPN complex corresponds to the M**ADP•P$_i$ state, ATPN will also be released from the pentacoordinated state with an unbroken $\beta-\gamma$ bond when the protein is denatured (*7*) and the similarity between the rate constants for the transitions from the open to the M**ATPN and to the M**ADP•P$_i$ states would not be a coincidence but could be specific for this transition.

The first detectable step in the association of actin and M**ATPN is an AM**ATPN state. According to the hypothesis of a pentacoordinated γP$_i$, this state is likely to be relatively stable. The measurements with ATPN and mantATPN suggest a value of $k_{-3'}$ (corresponding to k_{-3} in the equilibrium without actin bound) of at least <0.1 s^{-1} and values for $k_{3'}$ in the range of 0.002−0.5 s^{-1} (Table 3). These values can be compared with published data for the transition of the AM*ATP to the AM**ADP•P$_i$ state. These vary for the analogous k'_{-3} between 7 s^{-1} (*19*) and 5 s^{-1} (*20*) and for the corresponding k'_3 between 0.7 s^{-1} (*19*) and 50 s^{-1} (the latter value was given for the "attached" state; ref *20*). These data on ATP suggest that the binding of actin to the ADP•P$_i$ state has little effect on k_{-3} (which is about 10 s^{-1} in the absence of actin) while k_3 may be smaller in the actomyosin complex ($k_3 = 100$ s^{-1} in the absence of actin). These results are in qualitative agreement with the behavior of ATPN and are consistent with the hypothesis of an analogy between the M**ATPN and M**ADP•P$_i$ state.

The low value of k_{-3} (Scheme 2) causes the M**ATPN complex with actin to be an essential intermediate in the association of actin and S1−ATPN, as could be demonstrated by simulations using data from Table 3 (not shown), while in the dissociation a substantial part of the reaction pathway follows steps 3′ and 3 due to the small $k_{4'}$ and despite the very small value of $K_{3'}$. The question remains whether any particular feature of the mechanism is responsible for the strikingly slow rate of dissociation, which is smaller by a factor of more than 10 than for the isomeric AMPPNP (0.5 versus 15 s^{-1}; ref *21*). One limiting step, namely, the small $k_{4'}$, can be seen as resulting from the virtual absence of a fast equilibrium between open and closed states (*7*). The equilibrium between AM*N and AM**N is probably of little significance in the dissociation with ATP (*2*, *3*), while the AM**ATPN complex is an essential species in the interaction of myosin and actin with ATPN.

Table 3 includes only ranges of values for the rate constants for the interaction of myosin, actin, and ATPN. More exact values of the rate constants are not available for the present data. It should be noted that the values of some of these constants are not precisely known even for ATP.

The use of the tryptophan fluorescence as a signal in stopped-flow experiments with mantATPN, as presented in this work, gives information about both the binding process of mantATPN and the open → closed transition. The latter information was not available from the mant fluorescence signal as was assumed in experiments with mantATP (*8*). The quenching of the tryptophan fluorescence precedes the change in the mant signal on binding. An explanation may be that the fluorescence of the mant label is sensitive only to changes within its immediate surroundings, while the quench effect may be effective over longer distances: the tryptophan fluorescence could be quenched even in an initial state in which the mant label is less specifically bound, while the mant fluorescence changes only in response to the local interactions characteristic of the final specific binding.

An experimental limit in using the mant fluorescence as a signal is the increasing background and the corresponding decrease of the relative amplitude of the signal at higher concentrations, limiting the usable concentration to about 150 μM (*8*). In contrast, the amplitude of the quenching signal was at least theoretically independent of the concentration.

The limiting factor here was the light absorption by the label, which weakens the exciting light beam and caused the high noise. Limitations of the method described result from the finding that the quenching effect was not exclusively correlated with the binding process but accompanies the open → closed transition also, as implied by the experiments with *Dictyostelium* myosin. This factor, together with a small contribution due to the unavoidable inhomogeneity of mant nucleotides, may be responsible for the relative high variance of the values obtained, even in individual experiments. The efficient use of this method may depend on the availability of sufficient independent data for constraints and for independent checks.

The values measured for the dissociation and association of actoS1 and actin and S1 display a large variance which is in part due to the small number of experiments. A further reason may be the nonlinear relation between the light scattering signal and the concentration of actoS1 (according to ref *17* and to experiments described here) and nonspecific aggregation phenomena between actin and actoS1 (*16*). The latter may be responsible for the appearance of a shoulder in the trace of light scattering on dissociation of actoS1 in the presence of excess actin, which led Woodward et al. to propose a second slowly dissociating actoS1−mantADP species (*8*). This phenomenon did not depend on the presence of nucleotide, and there was no correlation between the change of mant fluorescence and the disappearance of this shoulder in the reaction with ATP. These results speak against the interpretation of Woodward et al. but do not invalidate the concept of "rigor" and attached states (*8*).

In summary, this study demonstrates that the use of ATPN provides experimental access to S1 and actoS1 states with myosin in the closed conformation, which are not accessible by other nucleotide analogues.

ACKNOWLEDGMENT

I thank Ken Holmes for interest and support and John Wray for encouraging discussions and for comments on the manuscript. I am grateful to Jochen Reinstein for advice on kinetics and to Georgios Tsiavaliaris for supplying the *Dictyostelium* protein. Phalloidin was a gift from the late Theodor Wieland.

REFERENCES

1. Geeves, M. A., and Holmes, K. C. (1999) Structural mechanism of muscle contraction, *Annu. Rev. Biochem. 68*, 687−728.
2. Urbanke, C., and Wray, J. (2001) A fluorescence temperature-jump study of conformational transitions in myosin subfragment 1, *Biochem. J. 358*, 165−173.
3. Málnási-Csizmadia, A., Pearson, D. S., Kovács, M., Woolley, R. J., Geeves, M. A., and Bagshaw, C. R. (2001) Kinetic resolution of a conformational transition and the ATP hydrolysis step using relaxation methods with a *Dictyostelium* myosin II mutant containing a single tryptophan residue, *Biochemistry 40*, 12727−12737.
4. Geeves, M. A., and Holmes, K. C. (2005) The molecular mechanism of muscle contraction, *Adv. Protein Chem. 71*, 161−193.
5. Lymn, R. W., and Taylor, E. W. (1971) Mechanism of adenosine triphosphate hydrolysis by actomyosin, *Biochemistry 10*, 4617−4624.
6. Mishenina, G. F., Samukov, V. V., and Shubina, T. N. (1979) Selective modification of monosubstituted phosphate groups in nucleoside and oligonucleotide 5′mono- and polyphosphates, *Bioorg. Khim. 5*, 886−894.
7. Wray, J., and Jahn, W. (2002) γ-amido ATP stabilizes a high fluorescence state of myosin subfragment 1, *FEBS Lett. 518*, 97−100.
8. Woodward, S. K. A., Eccleston, J. F., and Geeves, M. A. (1991) Kinetics of the interaction of 2′(3′)-*O*-(*N*-methylanthraniloyl)-ATP with myosin subfragment 1 and actomyosin subfragment 1: Characterization of two Acto·S1·ADP complexes, *Biochemistry 30*, 422−430.
9. Hiratsuka, T. (1983) New ribose-modified fluorescent analogs of adenine and guanine nucleotides available as substrates for various enzymes, *Biochim. Biophys. Acta 742*, 496−508.
10. Málnási-Csizmadia, A., Woolley, R. J., and Bagshaw, C. R. (2000) Resolution of conformational states of dictyostelium myosin II motor domain using tryptophan (W501) mutants: Implications for the open-closed transition identified by crystallography, *Biochemistry 39*, 16135−16146.
11. Geeves, M. A. (1989) Dynamic interaction between actin and myosin subfragment1 in the presence of ADP, *Biochemistry 28*, 5864−5871.
12. Siemankowski, R. F., and White, H. D. (1984) Kinetics of the interaction between actin, ADP and cardiac myosin-S1, *J. Biol. Chem. 259*, 5045−5053.
13. Conibear, P. B. (1999) Kinetic studies on effects of ADP and ionic strength on the interaction between myosin subfragment-1 and actin: Implications for load-sensitivity and regulation of the crossbridge cycle, *J. Muscle Res. Cell Motil. 20*, 727−742.
14. Kurzawa, S. E., and Geeves, M. A. (1996) A novel stopped flow method for measuring the affinity of actin for myosin head fragments using microgram quantities of protein, *J. Muscle Res. Cell Motil. 17*, 669−676.
15. Criddle, H., Geeves, M. A., and Jeffries, T. (1985) The use of actin labelled with *N*-(1-pyrenyl)iodoacetamide to study the interaction of actin with myosin subfragments and troponin/tropomyosin, *Biochem. J. 232*, 343−349.
16. Ando, T., and Scales, D. (1985) Skeletal muscle myosin subfragment-1 induces bundle formation by actin filaments, *J. Biol. Chem. 260*, 2321−2327.
17. Blanchoin, L., Didry, D., Carlier, M.-F., and Pantaloni, D. (1996) Kinetics of association of myosin subfragment-1 to unlabeled and pyrenyl-labeled actin, *J. Biol. Chem. 271*, 12380−12386.
18. Cremo, C. R., Neuron, J. M., and Yount, R. G. (1990) Interaction of myosin subfragment 1 with fluorescent ribose-modified nucleotides. A comparison of vanadate trapping and SH_1-SH_2 cross-linking, *Biochemistry 29*, 3309−3319.
19. White, H. D., Belknap, B., and Webb, M. R. (1997) Kinetics of nucleoside triphosphate cleavage and phosphate release steps by associated rabbit skeletal actomyosin, measured using a novel fluorescent probe for phosphate, *Biochemistry 36*, 11828−11836.
20. Smith, D. A., and Geeves, M. A. (1995) Strain-dependent cross-bridge cycle for muscle, *Biophys. J. 69*, 524−537.
21. Konrad, M., and Goody, R. (1982) Kinetic and thermodynamic properties of the ternary complex between F-actin, myosin subfragment 1 and adenosine 5′-[β,γ-imido]triphosphate, *Eur. J. Biochem. 128*, 547−555.

BI700318T